

DIFFUSER AUGMENTED WIND TURBINE FOR LOW-SPEED WIND

MOHAMED MOHAMED TAKEYELDEIN ELSHERBEINY

A thesis submitted in fulfilment of the
requirements for the award of the degree of
Doctor of Philosophy

School of Mechanical Engineering
Faculty of Engineering
Universiti Teknologi Malaysia

JUNE 2022

DEDICATION

Dedicated to Nadia Atwa, Mohamed Elsherbeiny, Ayman, Aya, and Amber

ACKNOWLEDGEMENT

All praises to Allah for getting me to this point in my Ph.D. journey. The author is grateful for the help and guidance from supervisors, especially Dr. Iskandar Shah Ishak, Dr. Tholudin Mat Lazim, and Dr. Nik Ahmad Ridhwan. They have been patient with the slow progress and are sincerely willing to share their knowledge.

The author is thankful for the help from friends, especially Essam Abubakar, Basem Aboutaleb, and Ismail AL Badawi; without their support, this research would not have been finished.

Thanks to all UTM Aerolab staff, especially Mr. Basid, Mr. Akmal, Mr. Salahuddin, and Mr. Mahathir. Especial thanks to Mr. Imran, Mr. Hing, and Mr. Iskandar Jema'in for helping the author fabricate his model. The author is also indebted to any individual who helped him through the conduction of this research.

ABSTRACT

Wind energy is the cheapest way to create additional renewable electric generating capacity. Nonetheless, it is proportional to the cubic of wind speed, which means that regions with low wind speeds, such as countries near the equator, have limited wind energy potential. Such limitation can be addressed with Diffuser Augmented Wind Turbine (DAWT), which can accelerate the flow and increase the efficiency of the wind turbine to exceed the Betz limit. However, the flow separation that occurs on the inner walls of DAWT is the main problem in degrading the DAWT performance. Furthermore, the flow is vulnerable to laminar separation at low wind speeds. Therefore, this study aimed to develop a DAWT that can operate at wind speeds lower than 5 m/s and investigate the possibility of using the number of rotor blades as a passive boundary layer control. The design of DAWT was developed by designing a bare wind turbine and a diffuser suitable for low wind speeds. The thin airfoil SD2030 was used as the blade profile of the bare turbine, while the suction surface of the same airfoil was also used as the profile of the diffuser to overcome laminar separation. In addition, the diffuser design was completed following a parameter study that evaluated flange configuration and height, diffuser cross-section profile, and diffuser opening angle. The final diffuser configuration has a flat flange with a height to rotor diameter ratio of 0.05 to minimize the total reference area of DAWT. Velocity vector analysis revealed that employing the suction surface of the airfoil SD2030 as the diffuser cross-section profile improved the flow structure by delaying stall at a wider opening angle, allowing the opening angle to be extended to 15°. After finalizing the DAWT design and its parameters, the effects of the rotor's blade numbers and solidity were evaluated by studying the 2-blade, 3-blade, and 4-blade DAWT. This research was conducted using computational fluid dynamics (CFD) simulations with Ansys CFX. Eventually, the final design was tested in a wind tunnel to validate the CFD results. The test findings show that the developed 3-blade DAWT has a low starting speed of 1m/s and effectively operates with a power coefficient of 0.599 at a low wind speed of 5m/s, which agrees with CFD results. By analyzing the velocity contours behind the rotor's plane, it was found that increasing the number of the rotor's blades increased the kinetic energy at the rotor's tips which helped energize the flow close to the diffuser's inner walls. Consequently, this helped the boundary layer stay attached to the diffuser's walls and avoid separation. Velocity vectors from CFD results showed that the 4-blade DAWT has the flow fully attached to the diffuser at an opening angle of 20° compared to the 3-blade and 2-blade DAWT, which had the flow completely separated at the same opening angle. These results proved that the rotor's blade number can be used as a passive boundary layer control. In conclusion, a DAWT which is suitable for low wind speeds has been successfully developed, benefiting nations with low average wind speeds like Malaysia. The potential of rotor's blade number as a passive boundary layer control has also been successfully investigated, which contributed to broadening the DAWT's understanding.

ABSTRAK

Tenaga angin adalah cara termurah untuk menghasilkan kapasiti penjanaan elektrik tambahan yang dapat diperbaharui. Tetapi, tenaga angin adalah berkadar dengan kelajuan angin kuasa tiga yang mana kawasan dengan kelajuan angin rendah seperti negara-negara berhampiran khatulistiwa, mempunyai potensi tenaga angin yang terhad. Kekangan ini mampu diatasi dengan Turbin Angin Tambahan Peresap (DAWT) yang berupaya untuk mempercepatkan dan meningkatkan kecekapan turbin angin melebihi had Betz. Walau bagaimanapun, pemisahan aliran yang berlaku pada dinding dalaman DAWT adalah masalah utama yang menjejaskan prestasi DAWT. Tambahan pula, aliran udara terdedah kepada pemisahan lamina pada kelajuan angin yang rendah. Oleh itu, kajian ini bertujuan untuk membangunkan DAWT yang boleh beroperasi pada kelajuan angin lebih rendah daripada 5m/s dan menyiasat kemungkinan untuk menggunakan bilangan bilah pemutar sebagai kawalan lapisan sempadan pasif. Reka bentuk DAWT telah dibangunkan dengan mereka bentuk turbin angin kosong dan peresap yang sesuai untuk kelajuan angin rendah. Kerajang udara nipis SD2030 digunakan sebagai profil bilah turbin kosong tersebut, sementara permukaan sedutan bagi kerajang udara yang sama juga digunakan sebagai profil peresap untuk mengatasi pemisahan lamina. Reka bentuk peresap merangkumi kajian parameter untuk menilai konfigurasi bebibir dan ketinggian, profil keratan rentas, dan sudut bukaan peresap. Konfigurasi akhir peresap mempunyai nisbah ketinggian bebibir berbanding diameter pemutar dengan nilai 0.05 untuk meminimumkan jumlah keluasan kawasan rujukan DAWT. Analisis vektor halaju menunjukkan bahawa profil peresap SD2030 telah melengahkan tegun pada sudut bukaan setinggi 15°. Selepas memuktamadkan reka bentuk DAWT dan parameternya, kesan nombor bilah pemutar dan kepejalannya dinilai dengan mengkaji DAWT 2-bilah, 3-bilah dan 4-bilah. Penyelidikan ini dijalankan menggunakan simulasi pengiraan dinamik bendalir (CFD) dengan Ansys CFX. Akhirnya, reka bentuk akhir telah diuji dalam terowong angin untuk mengesahkan keputusan CFD. Penemuan ujian menunjukkan bahawa DAWT 3 bilah yang dibangunkan mempunyai kelajuan permulaan yang rendah iaitu 1m/s dan berkesan beroperasi dengan pekali kuasa 0.599 pada kelajuan angin serendah 5m/s, konsisten dengan keputusan CFD. Dengan menganalisis kontur halaju di belakang satah pemutar, didapati bahawa menaikkan bilangan bilah rotor dapat meningkatkan tenaga kinetik pada hujung pemutar yang membantu memberi tenaga aliran dekat dengan dinding dalam peresap. Seterusnya ia membantu lapisan sempadan kekal melekat pada dinding peresap dan elakkan pemisahan. Vektor halaju daripada keputusan CFD menunjukkan bahawa DAWT 4-bilah mempunyai aliran yang melekat sepenuhnya pada peresap pada sudut bukaan 20° berbanding DAWT 3-bilah dan 2-bilah, yang mempunyai aliran dipisahkan sepenuhnya pada sudut bukaan yang sama. Keputusan CFD ini membuktikan bahawa nombor bilah pemutar boleh digunakan sebagai kawalan lapisan sempadan pasif. Kesimpulannya, reka bentuk DAWT yang sesuai untuk angin berkelajuan rendah telah berjaya dibangunkan, memberi manfaat kepada negara-negara yang mempunyai kelajuan angin purata rendah seperti Malaysia. Potensi bilangan bilah rotor sebagai kawalan lapisan sempadan pasif juga telah berjaya diselidiki, yang menyumbang untuk memperluas pemahaman DAWT.

TABLE OF CONTENT

	TITLE	PAGE
	DECLARATION	iii
	DEDICATION	iv
	ACKNOWLEDGEMENT	v
	ABSTRACT	vi
	ABSTRAK	vii
	TABLE OF CONTENT	viii
	LIST OF TABLES	xii
	LIST OF FIGURES	xiv
	LIST OF ABBREVIATIONS	xx
	LIST OF SYMBOLS	xxi
	LIST OF APPENDICES	xxii
CHAPTER1	INTRODUCTION	1
1.1	Introduction	1
1.1	Problem Statement	3
1.2	Objectives	4
1.3	Scope	4
CHAPTER 2	LITERATURE REVIEW	5
2.1	Available power in wind	5
2.2	Variable area ducts to speed up the flow.	6
2.2.1	Nozzles	6
2.2.2	Diffusers	7
2.3	Diffuser augmented wind turbines (DAWT)	9
2.4	Advantages of DAWT	10
2.5	Parameters that influence DAWT performance	11
2.5.1	Area ratio, opening angle, and length-to-diameter ratio	11
2.5.2	Diffuser profile	22
2.5.3	Backpressure (Flange)	25

2.5.4	The rotor effect (Number of the blades and solidity)	27
2.5.5	A network configuration of DAWT	29
2.6	DAWT power coefficient	30
2.7	DAWT at 5 m/s	31
2.8	CFD: various turbulence models to solve the DAWT problem	32
2.9	Airfoils for Wind Turbines	33
2.10	Airfoils for wind turbines at a low Reynolds number	33
2.11	Summary of literature review	34
CHAPTER 3	DAWT DESIGN METHODOLOGY	37
3.1	Workflow of the research	37
3.2	Airfoil Selection	40
3.3	Initial bare turbine design	43
3.4	Final bare turbine design	45
3.4.1	RPM measurement of the final turbine	49
3.5	Initial DAWT configuration	51
3.6	Parametric study of the diffuser-shroud	52
3.7	Final DAWT configuration (final diffuser design)	56
3.8	Multi blades of turbine's rotor	58
CHAPTER 4	METHODOLOGY	
	(CFD and WIND TUNNEL TESTING)	59
4.1	CFD	59
4.1.1	Validation	60
4.1.2	2D CFD simulation of SD2030 airfoil	61
4.1.3	Computational domain description	62
4.1.4	Grid sensitivity	64
4.2	Wind tunnel Testing	67
4.2.1	Blockage correction	69
CHAPTER 5	RESULTS AND DISCUSSIONS	71
5.1	Airfoil SD2030 curves using 2D CFD	71

5.2	Velocity contours of airfoil SD2030	72
5.3	Performance of the bare turbine using CFD	74
5.4	Performance of the initial diffuser (without a rotor)	74
5.5	Performance of a turbine with a flanged diffuser	76
5.6	Performance of turbine shrouded with a flange only	76
5.7	Pressure contours around a rotor attached to different shrouds	77
5.8	The initial DAWT performance with different opening angles	81
5.9	Position of the rotor relative to the diffuser	84
5.10	Multi-blade bare turbines (aspect ratio unchanged)	84
5.11	Multi-blade initial DAWT (aspect ratio unchanged)	85
5.12	Multi-blade initial DAWT vs. bare turbine (blade solidity unchanged)	88
5.13	The DAWT performance with a vortex generator as the flange	90
5.14	Effect of flange's height on the initial DAWT	91
5.15	Flat plate vs. airfoil-shaped diffuser cross-section profile	92
5.16	Performance of the final diffuser design (without a rotor)	95
5.17	Performance of the final DAWT design	97
5.18	Wind tunnel results of the four configurations	98
5.19	Upscaling the final DAWT to produce a power of 1 KW	101
5.20	Insights of flow separation inside the diffuser	103
	5.20.1 Comparison of the flow structure of the 3-blade DAWT and 2-blade DAWT at RPM 1100	107
5.21	Influence of the blade number on flow separation (using blade number as boundary layer controller)	108
CHAPTER 6	CONCLUSION AND RECOMMENDATIONS	111
6.1	Summary of findings	111

6.2	Conclusion	112
6.3	Contribution	112
6.4	Recommendations	113
REFERENCES		115
APPENDIX A DAWT FABRICATION PROCESS		125
LIST OF PUBLICATIONS		131

LIST OF TABLES

TABLE NO.	TITLE	PAGE
Table 2.1	A list of some shrouded turbine designs and their corresponding dimensions and performance.	21
Table 2.2	A list of some airfoils used as a diffuser cross-section in the literature.	24
Table 2.3	A list of the height of the flange used in some designs in the literature.	27
Table 2.4	A list of previous designs that use multi-blade rotors.	28
Table 2.5	A list of DAWT designs at 5 m/s.	31
Table 2.6	A review of various studies on various turbulence models to solve the DAWT problem.	32
Table 3.1	Three low Reynolds number airfoils are candidates as a blade profile.	42
Table 3.2	Geometry parameters of the initial rotor blade design.	45
Table 3.3	Geometry parameters of the final rotor design rotor designs.	47
Table 3.4.	Final bare turbine description.	48
Table 3.5	Initial diffuser geometrical description.	52
Table 3.6	A detailed description of the final diffuser.	57
Table 4.1	Torque value of the scaled NREL rotor at TSR 5.65 results from different mesh settings.	64
Table 4.2	Speed value at the diffuser inlet vs. first mesh element size adjacent to the diffuser.	66
Table 4.3	Torque value of the bare turbine vs. first mesh element size adjacent to the diffuser.	67
Table 4.4	Blockage ratio of the four configurations	69
Table 5.1	Lift and drag coefficient of SD2030 at AOA 2.17° using different turbulent models.	71

Table 5.2	The percentage increase in output torque of the DAWT at different opening angles.	84
Table 5.3	Maximum power of multi-blade DAWT (Aspect ratio unchanged).	87
Table 5.4	Maximum power of multi-blade DAWT (solidity unchanged).	89
Table 5.5	The percentage increase in output torque of the DAWT after replacing the flat plate flange with a vortex generator.	90
Table 5.6	Influence of the flange height variation on C_p of DAWT	92
Table 5.7	The influence of diffuser cross-section profile variation.	94
Table 5.8	The normalized power coefficient of the final DAWT.	98
Table 5.9	The startup speed of different configurations.	99
Table 5.10	The details of the up-scaled three-blade DAWT.	102
Table 5.11	The details of the up-scaled two-blade DAWT.	103
Table 5.12	Percentage of velocity deficit between the inlet and outlet planes.	105
Table 5.13	Maximum output power of the multiblade final DAWT.	109

LIST OF FIGURES

FIGURE NO.	TITLE	PAGE
Figure 1.1	Global Electricity Production End-2020 (1).	1
Figure 2.1	Available power in the wind per unit area.	5
Figure 2.2	Schematic diagram of a nozzle.	6
Figure 2.3	A smoke visualization of flow entering a nozzle conducted by Ohya et al. (9).	7
Figure 2.4	Pressure coefficient of the flow at the centerline of three different hollow structures tested by Ohya et al. (9).	8
Figure 2.5	A ratio between the flow velocity at the centerline and upstream velocity of three different hollow structures tested by Ohya et al. (9).	8
Figure 2.6	Wind lens turbine vs. bare wind turbine.	10
Figure 2.7	A relationship between the area ratio and the opening angle.	12
Figure 2.8	Length to diameter effect on the area ratio.	13
Figure 2.9	The opening angle effect on the area ratio.	13
Figure 2.10	The Vortec 7 DAWT, New Zealand (39).	14
Figure 2.11	Modification of Vortec 7 by Siavash et al.(40).	15
Figure 2.12	Results from the wind tunnel test conducted by Siavash et al. show an increase in power by 42.6% (40).	15
Figure 2.13	Results from an open field test conducted by Ohya et al. (41) show a 294% increase in power at 5 m/s.	16
Figure 2.14	Wind tunnel test results by Ohya et al.(41) show the normalized power coefficient of the shrouded turbine vs. the bare turbine at 6 m/s.	17
Figure 2.15	Results from the open field test conducted by Ohya et al. (24).show a 140% increase in power at 5 m/s.	17

Figure 2.16	Wind tunnel test results by Ohya et al. (24) show the normalized power coefficient of the shrouded turbine vs. the bare turbine at 8m/s.	18
Figure 2.17	CFD results of NREL turbine performance compared to NREL turbine shrouded with a compact diffuser(28).	19
Figure 2.18	Results from wind tunnel test conducted by Nunes et al. (28).	19
Figure 2.19	CFD results from Aranake et al.(10) show that the shrouded turbine has a high normalized power coefficient of 0.577.	20
Figure 2.20	Wind tunnel results of long convergent-divergent shrouded turbine conducted by Rivarolo et al. at 6.5 m/s (47).	22
Figure 2.21	Airfoil S1223 tested by Aranake et al. (10) using CFD compared to Airfoil SD1 developed by Leloudas et al. (48).	23
Figure 2.22	Airflow acceleration at the turbine plane vs. the relative radial position calculated using CFD (10,48).	23
Figure 2.23	Wind tunnel results conducted by Ohya et al. (24) show the flow acceleration achieved by a hollow diffuser with and without a flange.	25
Figure 2.24	Wind tunnel results conducted by Ohya et al. (24) show the flow acceleration achieved by a hollow diffuser with and without a flange.	26
Figure 2.25	Wind tunnel results from Ohya et al. show the effect of the flange height on the normalized power coefficient of the DAWT (24).	26
Figure 2.26	A unit circle contains five small circles.	29
Figure 2.27	A diagram shows the difference between the projected area of a bare turbine and a DAWT.	30
Figure 2.28	A general structure of a laminar separation bubble (8).	34
Figure 3.1	Workflow of the research.	39
Figure 3.2	S1223 airfoil is a high lift low Reynolds number airfoil with a cusped trailing edge (88).	41
Figure 3.3	A list of low Reynolds number airfoils.	42

Figure 3.4	The three airfoils listed in Table 3.1; are SD2030, SG6040, and E387 (17,87).	42
Figure 3.5	The drag knee at $Re=1 \times 10^5$ happened with SD2030 at a lower peak drag ($C_d < 0.02$) (16,87).	43
Figure 3.6	Initial rotor blade.	44
Figure 3.7	C_p -TSR curve of the initial rotor calculated using BEM (Qblade).	44
Figure 3.8	The taper distribution across the blade.	46
Figure 3.9	Torque-TSR curves of four blades with different taper distributions calculated using BEM (Qblade).	47
Figure 3.10	C_p -TSR curves of four blades with different chord distributions calculated using BEM (Qblade).	47
Figure 3.11	A technical drawing of the turbine rotor.	47
Figure 3.12	Reynolds number vs. blade's radial position at $TSR=4.3$.	49
Figure 3.13	Angle of attack (AOA) vs. the radial position at $TSR=4.3$.	49
Figure 3.14	The wind turbine model is fixed in the testing section of the UTM LST wind tunnel.	50
Figure 3.15	Maximum rotational speed of the final bare turbine at blade angle 5° .	50
Figure 3.16	Symmetrical schematic diagram of the initial diffuser.	51
Figure 3.17	A Technical drawing of the initial diffuser attached to the turbine and its dimensions.	51
Figure 3.18	DAWT's opening angle variation.	53
Figure 3.19	The relative position of the turbine's rotor to the diffuser.	54
Figure 3.20	The Diffuser's flange height variation.	54
Figure 3.21	The blade's number variation.	55
Figure 3.22	The flat plate flange is replaced by a co-rotating vortex generator with different angles.	55
Figure 3.23	A straight flange is replaced by a concave flange because it has a higher pressure drag coefficient.	56
Figure 3.24	The difference in pressure drags between concave shape and flat plate (93,94).	56
Figure 3.25	A Technical Drawing of the three-blade DAWT.	58
Figure 3.26	The 3-blade DAWT vs. the 2-blade DAWT.	58

Figure 4.1	Methods used to solve wind turbines performance.	59
Figure 4.2	Comparison between CFD results and Wind tunnel results from the literature.	61
Figure 4.3	Drag polar of Sd2030 airfoil evaluated by wind tunnel test conducted by Selig et al. (16).	62
Figure. 4.4	Computational grid for the shrouded turbine.	63
Figure. 4.5	Yplus contours at the diffuser surface.	65
Figure. 4.6	Yplus contours at the blade surface.	66
Figure 4.7	Front view of the test rig inside the wind tunnel testing section.	68
Figure 4.8	A side view of the 3-blade bare turbine shows the torque sensor and the brake disk used during the test.	69
Figure 5.1	Drag curve of SD2030 airfoil evaluated by different turbulence models, Xfoil, and wind tunnel test conducted by Selig et al. (16).	72
Figure 5.2	Lift curve of SD2030 airfoil evaluated by different turbulence models, Xfoil, and wind tunnel test.	72
Figure 5.3.	Velocity contour around SD2030 airfoil at AOA 2.17° evaluated by three different turbulence models.	73
Figure 5.4	The bare turbine output torque at an upstream speed of 5m/s.	74
Figure 5.5	The power coefficient curve of the bare turbine.	74
Figure 5.6	Performance of the initial diffuser configuration.	75
Figure 5.7	Velocity contours of the initial diffuser configuration.	75
Figure 5.8	Bare turbine vs. DAWT performance at upstream speed 5 m/s.	76
Figure 5.9	Turbine shrouded with a flange only behind the turbine section.	77
Figure 5.10	Pressure contours of the flow across the turbine plane.	79
Figure 5.11	Velocity vectors of the flow (flange only cases).	80
Figure 5.12	The torque of bare turbine vs. turbine shrouded with flanged-ring (flange at the front).	81
Figure 5.13	The torque of bare turbine vs. shrouded turbine (flange at the front).	81

Figure 5.14	DAWT performance at different opening angles.	83
Figure 5.15	Torque sensitivity to the opening angle at different RPM.	83
Figure 5.16	Augmentation ratio of DAWT at a different opening angle at high RPM (higher than the RPM at the peak torque).	83
Figure 5.17	Torque vs. RPM of multi-blade bare turbines.	85
Figure 5.18	Torque vs. RPM of multi-blade DAWT (Aspect ratio unchanged).	87
Figure 5.19	Augmentation ratio of a multi-blade DAWT (Aspect ratio unchanged).	87
Figure 5.20	Torque vs. RPM of 3-blade bare turbine vs. 6-blade bare turbine (solidity the same).	89
Figure 5.21	Torque vs. RPM of 3-blade DAWT vs. 6-blade bare turbine (solidity the same).	89
Figure 5.22	Torque vs. RPM of the DAWT after replacing the flat plate flange with a vortex generator.	91
Figure 5.23	Velocity vector across the DAWT (flat plate) at RPM 700 and opening angles of 10°.	93
Figure 5.24	Velocity vector across the DAWT (SD2030) at RPM 700 and opening angles of 10°.	93
Figure 5.25	Velocity vector across the DAWT (flat plate profile) at RPM 700 and opening angles of 15°.	94
Figure 5.26	Velocity vector across the DAWT (SD2030 profile) at RPM 700 and opening angles of 15°.	94
Figure 5.27	Velocity vector across the DAWT (cycloid profile) at RPM 700 and opening angles of 15°.	94
Figure 5.28	Performance of the final diffuser configuration.	96
Figure 5.29	Velocity contours of the final diffuser configuration.	96
Figure 5.30	Power coefficient vs. TSR curve of both the final DAWT (3-blade vs. 2-blade).	98
Figure 5.31	Power coefficient curves for the four configurations.	100
Figure 5.32	Velocity vectors and flow separation (3-blade DAWT vs. 2-blade DAWT).	104
Figure 5.33	Velocity deficit between inlet and outlet planes.	106
Figure 5.34	Velocity contours at the blade tip.	108

LIST OF ABBREVIATIONS

CFD	-	Computational Fluid Dynamics
DAWT	-	Diffuser Augmented Wind Turbine
BEM	-	Blade Element Momentum
RANS	-	Reynolds Averaged Navier Stokes
TSR	-	Tip Speed Ratio
RPM	-	Rotation Per Minute
Re	-	Reynolds Number
BL	-	Boundary Layer
SST	-	Shear Stress Transport
KKL	-	Koo Kleinstreuer Li

LIST OF SYMBOLS

C_p	-	Power Coefficient
C_p^*	-	Normalized Power Coefficient
θ	-	Diffuser opening angle
L	-	Diffuser length
D_e	-	Diffuser exit diameter
H	-	Flange height
r	-	Augmentation ratio
W	-	Watt
B_R	-	Blockage ratio
Y_{plus}	-	Non-dimensional distance

LIST OF APPENDICES

APPENDIX	TITLE	PAGE
Appendix A	DAWT fabrication process	125

CHAPTER1

INTRODUCTION

1.1 Introduction

Wind energy is one of the fastest expanding sources of new energy capacity. In 2020, the globe generated 743 GW of electricity (1), accounting for 6% of global production. Wind energy production increased by 93 GW compared to 2019, with an almost 14% growth rate. Many nations, such as Denmark, achieved 20% wind energy output, with wind energy accounting for 57 % of total power generation in 2019. (2). Figure 1.1 shows the share of renewable energy in the world's electricity production by 2020.

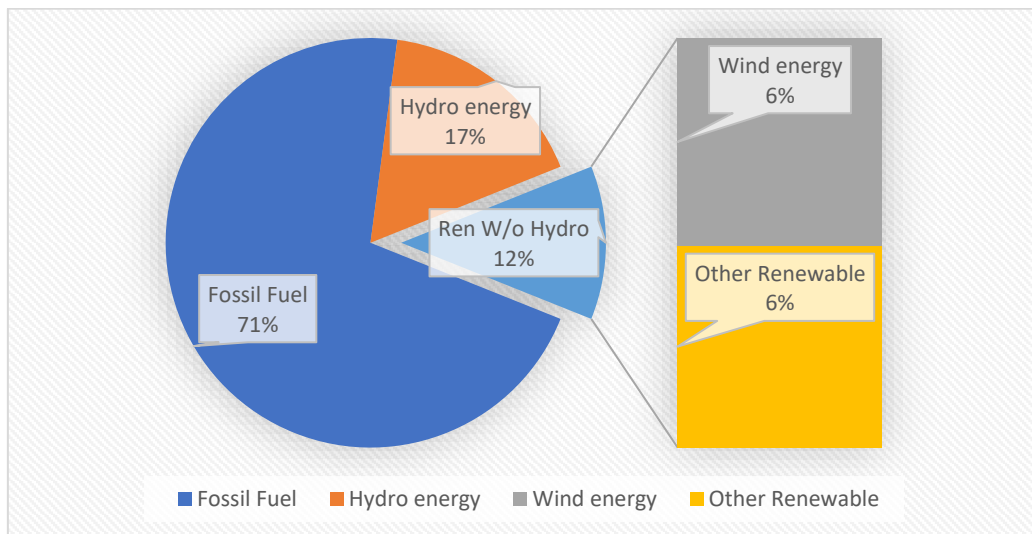


Figure 1.1 Global Electricity Production End-2020 (1).

Countries located in the equatorial zone, such as Malaysia, considered one of the Doldrums countries (located slightly to the north of the equator), are characterized by frequent showers, thunderstorms, heavy rainfall, and light wind speed. Malaysia's average offshore wind speed is between 1.2 m/s to 4.1 m/s, while many regions

worldwide have an average wind speed of 10 m/s (3–6). The East Coast of Peninsular Malaysia has the highest potential, with an annual resultant wind speed vector of 4.1 m/s (6). In the wind energy equation, wind speed is essential. The wind power is proportional to the cube of the wind speed and the square of the blade's diameter (7), as shown in Equation 1.1. Thus, countries with low wind speeds might have limited wind energy potential.

$$P = \frac{1}{2} \rho V^3 A \quad \text{Equation (1.1)}$$

Diffuser ducts have been proved to speed up the airspeed in a free flow by suction effect. A diffuser is a duct that serves pressure recovery (8); a pressure difference is created across its length. The diffuser inlet has a pressure lower than the atmosphere, encouraging the upstream air to flow through the diffuser (9).

The efficiency of wind turbines is limited to what is known by the Betz limit, which is 59.3% (7). Many researchers have demonstrated that adding a diffuser behind the turbine significantly increases power output, exceeding the Betz limit (10,11). Wind turbines shrouded with a diffuser are called diffuser augmented wind turbines (DAWT).

The diffuser increases the mass flow rate through the rotor. It causes a pressure gradient downstream after the rotor because the diffuser must end up with Sub-atmospheric pressure at its exit; the pressure directly behind the rotor is decreased. Hence, the pressure difference across the turbine increases, which increases the speed of air and hence the power(12,13). Diffuser augmented wind turbines (DAWT) have been proven to have enhanced performance compared to bare turbines at low wind speeds (10).

Two main parameters can increase the efficiency of the diffuser; the first one is increasing the area ratio between its inlet and outlet. However, increasing the area ratio is limited by the flow separation inside the diffuser walls. It was noticed that the turbine's wake mixed with the boundary layer shedding and reduced the separation (11,14). The second parameter is to decrease the exit pressure of the diffuser. Using

flanges at the exit of the diffuser creates vortex shedding behind it, which produces a low-pressure region at the diffuser exit (9,15).

The aerodynamics of DAWT turbines at low wind speed could be challenging because of the laminar separation that happens at a low Reynolds number. Airflow usually separates at a low Reynolds number below 5×10^5 , even though the boundary layer is still laminar and before the transition to turbulent. The laminar separation is usually accompanied by laminar separation bubbles, which cause extra drag force to the airfoil, known as the bubble drag (16,17).

1.1 Problem Statement

Diffuser Augmented wind turbines DAWT outperform bare turbines at low wind speeds. Flow separation happens at the inner walls of the diffuser walls because of the adverse pressure gradient. Laminar flow separation occurs at a low Reynolds number. Flow separation changes the effective shape of the diffuser, which limits its function. The number of the rotor's blades influences the energy and turbulent intensity of the wakes behind the turbine. The interaction between the turbine's wake and the flow passing inside the diffuser is critical to overall performance (14). There is insufficient knowledge about how the turbine's wake energy could be a factor in determining whether the flow separates the diffuser walls.

1.2 Objectives

The primary aim of the research is to develop a DWAT that can operate at low wind speed, which is conducted by achieving the following objectives:

1. To design a small horizontal axis wind turbine that can operate at low wind speeds.
2. To design a diffuser with a flange suitable for wind speeds below 5 m/s.
3. To evaluate the turbine's number of blades and the solidity impact on the flow separation inside the diffuser.
4. To investigate the possibility of using the number of rotor blades as a passive boundary layer control.

1.3 Scope

1. The influence of the geometrical parameter of the diffuser is investigated using 3D CFD simulation. The parameters studied are the flange height, turbine position, opening angle, and diffuser profile.
2. The optimum number of turbine blades that can help suppress the flow separation is investigated by studying 2-blade, 3-blade, and 4-blade rotors.
3. Wind tunnel testing is conducted for the prototype of the DAWT to measure the torque of the turbine using a torque sensor.

REFERENCES

1. REN21. Renewables 2021 Global Status Report. Paris: REN21 Secretariat; 2021. Report No.: 978-3-948393-00-8.
2. REN21. Renewables 2020 Global Status Report. Paris: REN21 Secretariat; 2020. Report No.: 978-3-948393-00-7.
3. Kadhem AA, Abdul Wahab NI, Abdalla AN. Wind Energy Generation Assessment at Specific Sites in a Peninsula in Malaysia Based on Reliability Indices. *Processes*. 2019;7(7):399.
4. Kadhem AA, Wahab NIA, Aris I, Jasni J, Abdalla AN. Advanced wind speed prediction model based on a combination of Weibull distribution and an artificial neural network. *Energies*. 2017;10(11):1744.
5. Islam MR, Saidur R, Rahim NA. Assessment of wind energy potentiality at Kudat and Labuan, Malaysia using Weibull distribution function. *Energy*. 2011;36(2):985–92.
6. Nor KM, Shaaban M, Abdul Rahman H. Feasibility assessment of wind energy resources in Malaysia based on NWP models. *Renewable Energy*. 2014;62:147–54.
7. Manwell JF, McGowan JG, Rogers AL. *Wind Energy Explained: Theory, Design and Application*, Second Edition. Hoboken, New Jersey: Wiley; 2009.
8. McLean D. *Understanding Aerodynamics: Arguing from the Real Physics*. Wiley-Blackwell; 2012.
9. Ohya Y, Karasudani T, Sakurai A, Inoue M. Development of a High-Performance Wind Turbine Equipped with a Brimmed Diffuser Shroud. *Transactions of the Japan Society for Aeronautical and Space Sciences*. 2006;49(163):18–24.
10. Aranake AC, Lakshminarayan VK, Duraisamy K. Computational analysis of shrouded wind turbine configurations using a 3-dimensional RANS solver. *Renewable Energy*. 2015;75:818–32.

11. Aranake AC, Lakshminarayan VK, Duraisamy K. Computational Analysis of Shrouded Wind Turbine Configurations. In: 51st AIAA Aerospace Sciences Meeting including the New Horizons Forum and Aerospace Exposition. Grapevine (Dallas/Ft. Worth Region), Texas: American Institute of Aeronautics and Astronautics; 2013.
12. Phillips DG, Flay RGJ, Nash TA. Aerodynamic Analysis and Monitoring of the Vortec 7 Diffuser-augmented Wind Turbine. In Wellington: Engineers New Zealand; 1998.
13. Bontempo R, Manna M. Performance analysis of open and ducted wind turbines. *Applied Energy*. 2014;136:405–16.
14. Toshimitsu K, Nishikawa K, Haruki W, Oono S, Takao M, Ohya Y. PIV measurements of flows around the wind turbines with a flanged-diffuser shroud. *Journal of Thermal Science*. 2008 Dec 1;17(4):375–80.
15. Ohya Y. Bluff body flow and vortex — its application to wind turbines. *Fluid Dynamics Research*. 2014;46(6):61423.
16. Selig MS, McGranahan BD. Wind Tunnel Aerodynamic Tests of Six Airfoils for Use on Small Wind Turbines; Period of Performance: October 31, 2002--January 31, 2003. 2004 Oct p. NREL/SR-500-34515, 15007930. Report No.: NREL/SR-500-34515, 15007930.
17. Selig MS, McGranahan BD. Wind Tunnel Aerodynamic Tests of Six Airfoils for Use on Small Wind Turbines. *Journal of Solar Energy Engineering*. 2004;126(4):986.
18. Anderson JD. Modern compressible flow with historical perspective. 4th Edition. Boston: McGraw-Hill.; 2021.
19. Klistafani Y, Mukhsen MI. Development of a Shrouded Wind Turbine with Various Diffuser Type Structures. *IOP Conference Series: Materials Science and Engineering*. 2019;676(1):012040.
20. Ohya Y, Karasudani T, Nagai T, Watanabe K. Wind lens technology and its application to wind and water turbine and beyond. *Renewable Energy and Environmental Sustainability*. 2017;2:2.
21. Igra. O. Shrouds for Aerogenerators. *Aiaa Journal*. 1976;14(10):1481–3.

22. Gilbert BL, Oman R a, Foreman KM. Fluid dynamics of diffuser-augmented wind turbines. *Journal of Energy*. 1978;2(6):368–74.
23. Gaden DLF, Bibeau EL. A numerical investigation into the effect of diffusers on the performance of hydro kinetic turbines using a validated momentum source turbine model. *Renewable Energy*. 2010;35(6):1152–8.
24. Ohya Y, Karasudani T. A shrouded wind turbine generating high output power with wind-lens technology. *Energies*. 2010;3(4):634–49.
25. Kosasih B, Tondelli A. Experimental Study of Shrouded Micro-Wind Turbine. *Procedia Engineering*. 2012 Jan 1;49:92–8.
26. Liu J, Song M, Chen K, Wu B, Zhang X. An optimization methodology for wind lens profile using Computational Fluid Dynamics simulation. *Energy*. 2016;109:602–11.
27. Lipian M, Dobrev I, Karczewski M, Massouh F, Jozwik K. Small wind turbine augmentation: Experimental investigations of shrouded- and twin-rotor wind turbine systems. *Energy*. 2019;186:115855.
28. Abdelwaly M, El-Batsh H, Bassily Hanna M. Numerical study for the flow field and power augmentation in a horizontal axis wind turbine. *Sustainable Energy Technologies and Assessments*. 2019;31:245–53.
29. Shahsavarifard M, Bibeau EL, Chatoorgoon V. Effect of shroud on the performance of horizontal axis hydrokinetic turbines. *Ocean Engineering*. 2015;96:215–25.
30. Kosasih B, Jafari SA. High-Efficiency Shrouded Micro Wind Turbine for Urban-Built Environment. *Applied Mechanics and Materials*. 2014;493:294–9.
31. Cresswell NW, Ingram GL, Dominy RG. The impact of diffuser augmentation on a tidal stream turbine. *Ocean Engineering*. 2015;108:155–63.
32. Wang WX, Matsubara T, Hu J, Odahara S, Nagai T, Karasutani T, et al. Experimental investigation into the influence of the flanged diffuser on the dynamic behavior of CFRP blade of a shrouded wind turbine. *Renewable Energy*. 2015;78:386–97.
33. Bontempo R, Manna M. Diffuser augmented wind turbines: Review and assessment of theoretical models. *Applied Energy*. 2020;280:115867.

34. Nunes MM, Brasil Junior ACP, Oliveira TF. Systematic review of diffuser-augmented horizontal-axis turbines. *Renewable and Sustainable Energy Reviews*. 2020 Nov;133:110075.
35. Shonhiwa C, Makaka G. Concentrator Augmented Wind Turbines: A review. *Renewable and Sustainable Energy Reviews*. 2016;59:1415–8.
36. Jabbar Al-Quraishi BA, Asmuin NZB, Mohd SB, Abd al-wahid WA, Mohammed AN, Didane DH. Review on Diffuser Augmented Wind Turbine (DAWT). *International Journal of Integrated Engineering*. 2019;11(1).
37. Watanabe K, Ohya Y. A Simple Theory and Performance Prediction for a Shrouded Wind Turbine with a Brimmed Diffuser. *Energies*. 2021 Jun 19;14(12):3661.
38. P.D.C Ten Hoopen. An Experimental and Computational Investigation of a Diffuser Augmented Wind Turbine [Master of Science Thesis]. TU Delft; 2009.
39. Flay RGJ. Model tests of wind turbines in wind tunnels. *Technical Transactions Budownictwo Zeszyt*. 2015 Dec 11;
40. Siavash NK, Najafi G, Hashjin TT, Ghobadian B, Mahmoodi E. An innovative variable shroud for micro wind turbines. *Renewable Energy*. 2020;145:1061–72.
41. Ohya Y, Karasudani T, Sakurai A, Abe K ichi, Inoue M. Development of a shrouded wind turbine with a flanged diffuser. *Journal of Wind Engineering and Industrial Aerodynamics*. 2008;96(5):524–39.
42. Ohya Y, Uchida T, Karasudani T, Hasegawa M, Kume H. Numerical Studies of Flow around a Wind Turbine Equipped with a Flanged-Diffuser Shroud Using an Actuator-Disk Model. *Wind Engineering*. 2012;36(4):455–72.
43. Takahashi S, Hata Y, Ohya Y, Karasudani T, Uchida T. Behavior of the Blade Tip Vortices of a Wind Turbine Equipped with a Brimmed-Diffuser Shroud. *Energies*. 2012;5(12):5229–42.
44. Abe K ichi, Ohya Y. An investigation of flow fields around flanged diffusers using CFD. *Journal of Wind Engineering and Industrial Aerodynamics*. 2004;92(3):315–30.

45. Nunes MM, Mendes RCF, Oliveira TF, Brasil Junior ACP. An experimental study on the diffuser-enhanced propeller hydrokinetic turbines. *Renewable Energy*. 2019 Apr;133:840–8.
46. Asl HA, Kamali Monfared R, Rad M. Experimental investigation of blade number and design effects for a ducted wind turbine. *Renewable Energy*. 2017 May;105:334–43.
47. Rivarolo M, Freda A, Traverso A. Test campaign and application of a small-scale ducted wind turbine with analysis of yaw angle influence. *Applied Energy*. 2020;279:115850.
48. Leloudas SN, Lygidakis GN, Eskantar AI, Nikolos IK. A robust methodology for the design optimization of diffuser augmented wind turbine shrouds. *Renewable Energy*. 2020;150:722–42.
49. Jafari SAH, Kosasih B. Flow analysis of shrouded small wind turbine with a simple frustum diffuser with computational fluid dynamics simulations. *Journal of Wind Engineering and Industrial Aerodynamics*. 2014;125:102–10.
50. Civalier G, Fridley C, Li J, Seabe J, Stanciu AX, Willey M, et al. Comparative Analysis of Three Concepts for Aerostat Based Electrical Power Generation System. In: 11th AIAA Aviation Technology, Integration, and Operations (ATIO) Conference. Virginia Beach, VA: American Institute of Aeronautics and Astronautics; 2011.
51. Shives M, Crawford C. Developing an empirical model for ducted tidal turbine performance using numerical simulation results. *Proceedings of the Institution of Mechanical Engineers, Part A: Journal of Power and Energy*. 2012;226(1):112–25.
52. Chen TY, Liao YT, Cheng CC. Development of small wind turbines for moving vehicles: Effects of flanged diffusers on rotor performance. *Experimental Thermal and Fluid Science*. 2012;42:136–42.
53. Mansour K, Meskinkhoda P. Computational analysis of flow fields around flanged diffusers. *Journal of Wind Engineering and Industrial Aerodynamics*. 2014;124:109–20.
54. Olasek K, Karczewski M, Lipian M, Wiklak P, Józwik K. Wind tunnel experimental investigations of a diffuser augmented wind turbine model. *International Journal of Numerical Methods for Heat and Fluid Flow*. 2016;26(7):2033–47.

55. Mühle F, Adaramola MS, Sretran L. The effect of the number of blades on wind turbine wake - a comparison between 2-and 3-bladed rotors. *Journal of Physics: Conference Series*. 2016;753:032017.
56. Toshimitsu K, Kikugawa H, Sato K, Sato T. Experimental Investigation of Performance of the Wind Turbine with the Flanged-Diffuser Shroud in Sinusoidally Oscillating and Fluctuating Velocity Flows. *Journal of the Japan Society of Mechanical Engineers*. 2012;2012(December):215–21.
57. Wang SH, Chen SH. Blade number effect for a ducted wind turbine. *Journal of Mechanical Science and Technology*. 2008;22(10):1984–92.
58. Riyanto, Pambudi NA, Febriyanto R, Wibowo KM, Setyawan ND, Wardani NS, et al. The Performance of Shrouded Wind Turbine at Low Wind Speed Condition. *Energy Procedia*. 2019;158:260–5.
59. Agha A, Chaudhry HN, Wang F. Determining the augmentation ratio and response behaviour of a Diffuser Augmented Wind Turbine (DAWT). *Sustainable Energy Technologies and Assessments*. 2020;37:100610.
60. Agha A, Chaudhry HN, Wang F. Diffuser Augmented Wind Turbine (DAWT) Technologies: A Review. *International journal of Renewable Energy Research*. 2018;8:1369–85.
61. Ohya Y, Watanabe K. A New Approach Toward Power Output Enhancement Using Multirotor Systems with Shrouded Wind Turbines. *Journal of Energy Resources Technology*. 2019;141(5):051203.
62. Hand MM, Simms DA, Fingersh LJ, Jager DW, Cotrell JR, Schreck S, et al. Unsteady Aerodynamics Experiment Phase VI: Wind Tunnel Test Configurations and Available Data Campaigns. Golden Colorado: National Renewable Energy Laboratory; 2001. Report No.: NREL/TP-500-29955, 15000240.
63. Sridhar S, Zuber M, B. SS, Kumar A, Ng EYK, Radhakrishnan J. Aerodynamic comparison of slotted and non-slotted diffuser casings for Diffuser Augmented Wind Turbines (DAWT). *Renewable and Sustainable Energy Reviews*. 2022 Jun;161:112316.
64. Alkhabbaz A, Yang HS, Tongphong W, Lee YH. Impact of compact diffuser shroud on wind turbine aerodynamic performance: CFD and experimental investigations. *International Journal of Mechanical Sciences*. 2022 Feb;216:106978.

65. Mann HS, Singh PK. Energy recovery ducted turbine (ERDT) system for chimney flue gases - A CFD based analysis to study the effect of number of blade and diffuser angle. *Energy*. 2020 Dec;213:118501.
66. Refaie AG, Hameed HSA, Nawar MAA, Attai YA, Mohamed MH. Comparative investigation of the aerodynamic performance for several Shrouded Archimedes Spiral Wind Turbines. *Energy*. 2022 Jan;239:122295.
67. Heragy M, Kono T, Kiwata T. Investigating the effects of wind concentrator on power performance improvement of crossflow wind turbine. *Energy Conversion and Management*. 2022 Mar;255:115326.
68. Ali QS, Kim MH. Quantifying impacts of shell augmentation on power output of airborne wind energy system at elevated heights. *Energy*. 2022 Jan;239:121839.
69. Ali QS, Kim MH. Power conversion performance of airborne wind turbine under unsteady loads. *Renewable and Sustainable Energy Reviews*. 2022 Jan;153:111798.
70. Bontempo R, Carandente R, Manna M. A design of experiment approach as applied to the analysis of diffuser-augmented wind turbines. *Energy Conversion and Management*. 2021 May;235:113924.
71. Dessoky A, Bangga G, Lutz T, Krämer E. Aerodynamic and aeroacoustic performance assessment of H-rotor darrieus VAWT equipped with wind-lens technology. *Energy*. 2019 May;175:76–97.
72. Gough H, King MF, Nathan P, Grimmond CSB, Robins A, Noakes CJ, et al. Influence of neighbouring structures on building façade pressures: Comparison between full-scale, wind-tunnel, CFD and practitioner guidelines. *Journal of Wind Engineering and Industrial Aerodynamics*. 2019 Jun;189:22–33.
73. Ramayee L, Supradeepan K, Ravinder Reddy P, Karthik V. Design of shorter duct for wind turbines to enhance power generation: a numerical study. *J Braz Soc Mech Sci Eng*. 2022 Apr;44(4):160.
74. Nur Shamimi Amirah Md Sunhazim, Fazila Mohd Zawawi, Ummikalsom Abidin, Syahrullail Samion, Kamarulafizam Ismail, Ainaa Maya Munira Ismail. CFD Investigation on The Jet-Engine Inspired Wind Turbine. *CFDL*. 2022 Mar 2;14(2):72–80.

75. Avallone F, Ragni D, Casalino D. On the effect of the tip-clearance ratio on the aeroacoustics of a diffuser-augmented wind turbine. *Renewable Energy*. 2020 Jun;152:1317–27.
76. Kim IH, Kim BR, Yang YJ, Jang SJ. Parametric Study on Ducted Micro Wind Energy Harvester. *Energies*. 2022 Jan 19;15(3):727.
77. Ranjbar MH, Rafiei B, Nasrazadani SA, Gharali K, Soltani M, Al-Haq A, et al. Power Enhancement of a Vertical Axis Wind Turbine Equipped with an Improved Duct. *Energies*. 2021 Sep 14;14(18):5780.
78. Grondeau M, Guillou S, Mercier P, Poizot E. Wake of a Ducted Vertical Axis Tidal Turbine in Turbulent Flows, LBM Actuator-Line Approach. *Energies*. 2019 Nov 9;12(22):4273.
79. Nojan, Bagheri-Sadeghi. Optimal Aerodynamic Design DESIGN of Ducted Wind Turbines [Doctor of Philosophy]. CLARKSON UNIVERSITY; 2021.
80. Tangler JL, Somers DM. NREL Airfoil Families for HAWTs. AWEA. 1995;1–12.
81. Tangler JL, Somers DM. NREL Airfoil Families for HAWTs. Golden Colorado: National Renewable Energy Laboratory; 1995 p. 1–12. Report No.: NREL/TP-442-7109.
82. Bertagnolio F, Sorensen NN, Johansen J, Fuglsang P. Wind turbine airfoil catalogue. Roskilde, Denmark: Risø National Laboratory; 2001. Report No.: Risø-R-1280 (EN).
83. Schubel PJ, Crossley RJ. Wind Turbine Blade Design. *Energies*. 2012 Sep 6;5(9):3425–49.
84. Snel H, Schepers JG, Montgomerie B. The MEXICO project (Model Experiments in Controlled Conditions): The database and first results of data processing and interpretation. *Journal of Physics: Conference Series*. 2007 Jul 1;75:012014.
85. Giguère P, Selig MS. Low Reynolds number airfoils for small horizontal axis wind turbines. *Wind Engineering*. 1997;21(6):367–80.
86. Singh RK, Ahmed MR, Zullah MA, Lee YH. Design of a low Reynolds number airfoil for small horizontal axis wind turbines. *Renewable Energy*. 2011;

87. Giguère P, Selig MS. New Airfoils for Small Horizontal Axis Wind Turbines. *Journal of Solar Energy Engineering*. 1998;120(2):108.
88. Selig MS, Guglielmo JJ. High-Lift Low Reynolds Number Airfoil Design. *Journal of Aircraft*. 1997;34(1):72–9.
89. Hsiao F bin, Bai C jeng, Chong W tong. The Performance Test of Three Different Horizontal Axis Wind Turbine (HAWT) Blade Shapes Using Experimental and Numerical Methods. *Energies*. 2013;6(6):2784–803.
90. Marten D, Wendler J. QBlade Guidelines v0.6. TU Berlin; 2013.
91. Çengel YA, Cimbala JM. *Fluid mechanics: fundamentals and applications*. Boston: McGraw-Hill Higher Education; 2006. 956 p. (McGraw-Hill series in mechanical engineering).
92. Anderson JD. *Fundamentals of aerodynamics*. Sixth edition. New York, NY: McGraw Hill Education; 2017. 1130 p. (McGraw-Hill series in aeronautical and aerospace engineering).
93. Bektas M. *Great Formulas Explained - Physics, Mathematics, Economics*. Independently Published; 2017.
94. Hoerner SF. *Fluid-dynamic drag: Practical information on aerodynamic drag and hydrodynamic resistance*. Albuquerque, N.M: Hoerner Fluid Dynamics.; 1965.
95. Cho T, Kim C. Wind tunnel test for the NREL phase VI rotor with 2m diameter. *Renewable Energy*. 2014;65:265–74.
96. Zidane IF, Swadener G, Saqr KM, Ma X, Mohamed F. CFD Investigation of Transitional Separation Bubble Characteristics on NACA 63415 Airfoil at Low Reynolds Numbers. In: *Proceedings of the 25th UKACM Conference on Computational Mechanics*. 2017.
97. Aftab SMA, Rafie ASM, Razak NA, Ahmad KA. Turbulence model selection for low reynolds number flows. *PLOS One*. 2016;11(4):e0153755.
98. Wiriadidjaja S, Hasim F, Mansor S, Asrar W, Rafie ASM, Abdullah EJ. Subsonic Wind Tunnels in Malaysia: A Review. *Applied Mechanics and Materials*. 2012;225:566–71.

99. Jeong H, Lee S, Kwon SD. Blockage corrections for wind tunnel tests conducted on a Darrieus wind turbine. *Journal of Wind Engineering and Industrial Aerodynamics*. 2018;179:229–39.
100. Cheng S, Jin Y, Chamorro LP. Wind Turbines with Truncated Blades May Be a Possibility for Dense Wind Farms. *Energies*. 2020 Apr 9;13(7):1810.

LIST OF PUBLICATIONS

Journal with Impact Factor

1. Takeyeldein MM, Lazim TM, Mohd NARN, Ishak IS, Efkiern EA. Wind Turbine Design Using Thin Airfoil SD2030. Evergreen. 2019;6(2):114–23. (Indexed by SCOPUS)
2. Takey M, Lazim TM, Ishak IS, Nik Mohd NAR, Othman N. Computational investigation of a wind turbine shrouded with a circular ring. CFD Lett. 2020;12(10):40–51. (Indexed by SCOPUS)
3. Takeyeldein MM, Lazim TM, Ishak IS, Nik Mohd NAR, Ali EA. Wind lens performance investigation at low wind speed. Evergreen. 2020;7(4):481–8. (Indexed by SCOPUS)